Temperature dependence of structure and density for D_2O confined in MCM-41-S

2012 J. Phys.: Condens. Matter 24 064106

(http://iopscience.iop.org/0953-8984/24/6/064106)

J. Phys.: Condens. Matter **24** (2012) 064106 (7pp) doi:10.1088/0953-8984/24/6/064106

Temperature dependence of structure and density for D_2O confined in MCM-41-S

William A Kamitakahara[1], Antonio Faraone[1,2], Kao-Hsiang Liu[3] and Chung-Yuan Mou[3]

[1] NIST Center for Neutron Research, National Institute of Standards and Technology, Gaithersburg, MD 20899, USA
[2] Department of Materials Science and Engineering, University of Maryland, College Park, MD 20742, USA
[3] Department of Chemistry, National Taiwan University, Taipei 106, Taiwan

Received 27 April 2011, in final form 1 August 2011
Published 25 January 2012
Online at stacks.iop.org/JPhysCM/24/064106

Abstract
Using neutron diffraction, we have tracked the temperature dependence of structural properties for heavy water confined in the nanoporous silica matrix MCM-41-S. By observing the correlation peak corresponding to the pore–pore distance, which is determined by the scattering contrast between the silica and the water, we monitored the density of the confined water. Concurrently, we studied the prominent first diffraction peak of D_2O at $\approx$1.8 $Å^{-1}$, which furnishes information on the microscopic arrangement of the water molecules. The data show the presence of a density maximum at $\approx$275 K ($\pm$10 K), a property similar to bulk water, and the occurrence of a density minimum at $\approx$180 K ($\pm$10 K). The prominent diffraction peak of D_2O is found to shift and sharpen over a wide T range from 200 to 270 K, reflecting structural changes that are strongly correlated with the changes in density. We also observe the continuous formation of external ice, arising from water expelled from the pores while expansion takes place within the pores. An efficient method for monitoring the density of the confined D_2O using a triple-axis spectrometer is demonstrated.

(Some figures in this article are in colour only in the electronic version)

1. Introduction

The behavior of hydration water and water in confinement remains the object of intense research, because of its relevance to many diverse areas, including biology, geology, and catalysis [1]. Porous silica glasses with cavities of nanometer dimensions offer convenient model systems for studies of confined water. Recently, much attention has been devoted to water confined in nanoporous MCM-41-S, in which the water resides in cylindrical channels arranged in a hexagonal geometry. In this material, the available pore diameters can range from $\approx$100 to $\approx$10 Å, with a very narrow pore size distribution within a given sample. It is noteworthy that, while bulk water cannot be supercooled below a homogeneous nucleation temperature (approximately 231 K for light water or 235 K for heavy water), confined water may crystallize at considerably lower temperatures, or not at all. In MCM-41-S, for pore diameters less than 20 Å, no freezing peak can be observed in a differential scanning calorimetry (DSC) measurement [2]. Thus, confining water within MCM-41-S allows exploration of the 'no man's land' [3], the region of the phase diagram below the homogeneous nucleation temperature where liquid bulk water cannot be obtained. However, the extent to which the properties of such confined water are related to those of bulk water is controversial, since the effect of the confining walls is difficult to estimate. Nonetheless, it may well be that the study of confined water in MCM-41-S may offer insights into cases where the environment of the water is influenced by close approach to a hydrophilic surface or site, i.e. many important systems in biology and chemistry.

Neutron and x-ray scattering methods figure prominently among the many techniques that have been applied to study water in confinement. Some of the participants in the current investigation (AF, CYM) have observed the relaxational dynamics of H_2O confined in MCM-41-S using quasielastic

neutron scattering, and reported a dynamic crossover in the diffusive motions at $T_L \approx 225$ K at ambient pressure [4]. The behavior was attributed to the crossing of the 'Widom line', the locus of the maximum correlation length in the *P–T* plane, emanating from a proposed liquid–liquid critical point of water [5]. The latter is envisaged as the end point of the first order transition line between the high density liquid water (HDL) and the low density liquid water (LDL), liquid counterparts of the high density amorphous ice (HDA) and low density amorphous ice (LDA), respectively [5, 6]. The hypothesis that bulk supercooled water can be considered a mixture of a high density form and a low density form was suggested by molecular dynamics (MD) simulations and has recently found experimental support from the results of x-ray experiments [7]. For water confined in MCM-41-S, crossing the Widom line entails a structural change from a predominantly high-density phase to a lower-density phase. This scenario arises from the investigation of infrared (IR) O–H bending bands [8]. Notwithstanding these and other [9] results in support of the hypothesis of the existence of a second critical point of water [10–12], this concept has attracted strong criticism [13–15] and remains controversial.

The structure of water confined in MCM-41 nanopores has been investigated previously by several other groups. Dore and co-workers have carefully studied the structure of D_2O confined in MCM with pore sizes ranging from ≈100 to ≈20 Å [16, 17]. Yoshida *et al* [18] have investigated samples with pore diameters of 28, 24, and 20 Å and reported the neutron diffraction pattern of D_2O at several temperatures in the range from 300 to 170 K, together with a study of the dynamics by neutron spin echo. Morishige *et al* [19] used x-ray diffraction to investigate the pore size and temperature dependence of H_2O structure in MCM-41 and porous silica glasses. Recently, by measuring the intensity of the Bragg diffraction peak arising from the (10) plane of the 2D hexagonal lattice of water cylinders in the MCM-41-S silica matrix, Liu *et al* [20] investigated the temperature dependence of the density of nanoconfined water and reported the location of a density minimum. The intensity of the Bragg peak arising from interpore correlations depends on the scattering length density contrast between the confined liquid (D_2O) and the matrix (silica), which is in turn determined by the density of water, and hence the latter can be determined. This method has been employed previously to investigate the density of confined toluene, benzene, and methanol [21–24]. Recently, Mancinelli *et al* [25] performed a detailed investigation of the microscopic structure of the water in the pores using a neutron diffractometer appropriate for liquid samples. Combining their experiments with computer simulations, they emphasized the existence of strong layering effects at the pore surfaces that affect the structure of water in the pores. They claim that such layering effects may significantly influence the intensity of the correlation Bragg peak, and also hypothesize the existence of voids within the otherwise water-filled pores.

The focus of the current experiment is to correlate changes in the main features in the diffraction pattern with changes in density and dynamics, using a triple-axis spectrometer (TAS). While the TAS is not an efficient instrument for collecting diffraction data on non-crystalline materials, we have found that, for D_2O in MCM-41-S, it offers a convenient and surprisingly effective means of monitoring the scattering profile within restricted *Q*-ranges that reflect pronounced structural changes. In our experiment, we directed our attention to the lowest-order (10) pore correlation Bragg peak and to the first sharp diffraction peak (FSDP) of the water structure factor. We performed our investigation in a temperature range from 290 to 160 K, at 10 K intervals for the FSDP, and much smaller steps for the low-*Q* correlation peak, thus detailing the temperature dependence with data similar to those reported at fewer temperatures by Yoshida *et al* [18] and Mancinelli *et al* [25]. Moreover, as we shall demonstrate, the samples we investigated were completely filled with D_2O, but not significantly over-filled. This provided us with the ability to monitor the amount of water expelled from the pores as temperature was lowered, and to relate it to the changes in density.

2. Experimental details

The sample of MCM-41-S was synthesized by methods described in previous experiments [20], which involved seeding with β-zeolite precursors [26]. Complete dehydration of the sample by heating in vacuum was followed by hydration with D_2O in a sealed glass container with an open source of D_2O to provide a saturated humidity environment at ambient temperature of about 294 K. The hydration was allowed to equilibrate over a period of two weeks, and the final hydration level was determined by measuring the mass gain. The dehydrated mass of the sample used for neutron scattering was 2.777 g, while the hydrated mass was 4.266 g, implying an uptake of (1.489 ± 0.005) g of D_2O and a fractional mass gain of 0.54. As shown in section 3.1, the pores in the sample thus hydrated are just filled, with a negligible amount of water outside the pores. This condition permits us to observe, as the water confined in the pores expands and expels some of the liquid, the continuous formation of crystalline ice Bragg peaks due to the expelled fraction. As far as the study of the FSDP is concerned, the presence, in the *Q* region of interest, of three Bragg peaks arising from ice outside the pores slightly complicates but does not otherwise affect the data analysis.

The sample was enclosed in a cylindrical thin-walled aluminum sample can with a diameter of 17 mm and a length of 55 mm. The neutron scattering measurements were carried out on a conventional thermal triple-axis spectrometer at the NIST Center for Neutron Research (NIST), employing a graphite monochromator and analyzer crystals to define an elastic energy window of 1.2 meV full width at half maximum (FWHM), with a resolution in the wavevector of 0.04 $Å^{-1}$ FWHM at $Q = 0.25$ $Å^{-1}$, and of 0.026 $Å^{-1}$ at $Q = 1.8$ $Å^{-1}$. A closed-cycle helium refrigerator allowed control of the sample temperature within 1 K.

The temperature dependence of the structure factor was measured in the *Q* ranges from 0.1 to 0.4 $Å^{-1}$ and from 1.0 to 2.4 $Å^{-1}$, in the temperature range from 160 to 280 K, taking data at 10 K steps. In addition, in order to monitor in detail

the temperature dependence of the density of confined D_2O, the instrument was set up to measure the scattered intensity at the (10) peak; then, the sample temperature was continuously ramped at 0.1 K min^{-1} while data were collected every 5 min. The ramp rate was chosen to be slow enough that the sample can be considered at equilibrium and free of internal gradients. This was confirmed by comparing with data using a ramp rate of 0.2 K min^{-1}, and verifying that, within the experimental uncertainties, the results were unchanged, when cooling and heating scans were averaged.

3. Results and discussion

3.1. Low Q data-derived density versus T

Figure 1 shows the low Q diffraction pattern between 0.1 and 0.4 Å^{-1} for the hydrated MCM-41-S sample at six representative temperatures, after empty can subtraction. The scans were fitted using the equation [13]:

$$I(Q) = AQ^{-\gamma} + B + K^2P(Q, r, L)L(Q, Q_0, \Gamma) \qquad (1)$$

where $P(Q, r, L)$ is the orientationally averaged form factor of a cylinder of radius r and length L and $L(Q, Q_0, \Gamma)$ is a Lorentzian function centered at Q_0 with a FWHM Γ. According to equation (1) three main components contribute to the pattern: (i) a power law decay; (ii) a peak centered at Q_0; (iii) a constant background. The power law decay originates from the Porod scattering of the silica grains and therefore γ_{PL} should be close to four, as expected for a smooth surface. The Lorentzian peak is the (10) plane Bragg peak and is modulated by the form factor of the cylindrical pores, $P(Q, r, L)$. Its intensity is proportional to the neutron scattering length density contrast between the silica matrix and the confined water:

$$K^2 = A(\rho_w - \rho_m)^2, \qquad (2)$$

where ρ_w and ρ_m are neutron scattering length density of the confined and confining phases, respectively. Finally, we account for other scattering expected from the silica and heavy water with a flat background B. The fitted value of γ, the power law decay exponent, is 2.4 ± 0.3, considerably smaller than the value of four expected from surface scattering, but the values obtained for the pore radius and the peak position, $Q_0 = 0.26$ Å^{-1} $\pm$ 0.01 Å^{-1}, correspond more closely to anticipated values. For the former, we obtained $r = 7.5$ Å ± 0.2 Å, apparently consistent with the nominal channel diameter of 16 Å, while for the latter, the fits gave $Q_0 = 0.26$ Å^{-1} $\pm$ 0.01 Å^{-1}, implying a mean distance between the cylindrical channels of $(4\pi/\sqrt{3})/0.26$ Å^{-1} $\approx$ 28 Å.

It has recently been pointed out by Soper [27] that the nominal channel diameter for MCM-41-S samples can be quite inconsistent with the observed water uptake. In our experiment, one would expect a maximum hydration mass gain of about 21% over the dry mass, assuming silica and D_2O densities of 2.2 g cm^{-3} and 1.04 g cm^{-3} respectively, and that the channel spacing is 28 Å and the channel diameter is 16 Å. The former is unlikely to be in serious error, deriving as it does from a peak position. If the channel diameter were somewhat larger, i.e. 21.2 Å, a mass gain of 54% would be possible, with all adsorbed water in the pores.

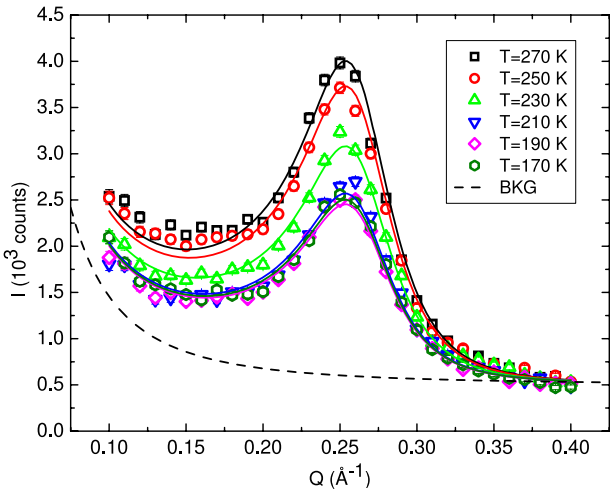

Figure 1. Diffraction from the low Q interpore correlation peak at representative temperatures. Error bars are standard deviations, determined by counting statistics, and are smaller than the symbols. Continuous lines represent the result of fitting, as described in the text. The dashed line represents the contribution from the incoherent background and Porod scattering.

Numerically, the relation between the scattering length density and the physical density of the adsorbed heavy water in g cm^{-3} is

$$\rho_w = 5.76 \times 10^{10} \text{ cm}^{-2} \times \rho_{hw}. \qquad (3)$$

If we assume that the channels maintain their dimensions and form in dehydrated MCM-41-S, it follows that

$$\rho_{hw} = (\rho_m/5.76 \times 10^{10} \text{ cm}^{-2})[(I_{wet}/I_{dry})^{1/2} + 1], \qquad (4)$$

where I_{wet} and I_{dry} are the observed intensities for hydrated and dry samples containing the same amount of silica. In this analysis, we assume that the MCM-41-S host consists of silica of uniform density, penetrated by channels filled with fluid of uniform density. While our assumptions may lead to uncertainties in ρ_{hw} that are difficult to estimate, we believe that they are not major sources of error. Equation (4) implies that the derived water density is not very sensitive to the value of I_{dry}, since taking the square root of the intensity ratio ($\approx$0.4) and adding unity means in practice that a 3% uncertainty in I_{dry} leads to only a 0.6% uncertainty in ρ_{hw}.

Thus, by making separate measurements on a dehydrated sample of the MCM-41-S material, we have obtained data on I_{dry} that are completely adequate for our purposes. By far the largest source of uncertainty in applying equation (4) arises from lacking accurate data on the silica scattering density ρ_m. This means our measurements are very precise in a relative sense, but the overall density scale has substantial uncertainty.

We are not assuming that the distribution of water in the pores is uniform, but that there is an average D_2O density that is reflected through the scattering length contrast between water and silica. That is, if the spatial distribution of absorbed

water changes only in scale, but not in functional form, our approach is valid. While others [25, 27] argue that a changing distribution as a function of temperature could be primarily responsible for the changes in the intensity of the low-Q diffraction peak, we believe that this is rather unlikely. In our view, an expansion of the occluded water while undergoing slow freezing into an amorphous state seems more physically reasonable to us than maintaining a constant density. Our observation of the expulsion of water on cooling is, we believe, strong evidence of our basic picture.

Several reports have been published that offer different estimates of the silica scattering density in MCM-41. Edler *et al* [28], analyzing SANS data on MCM-41 with 42 Å diameter channels filled with D_2O/H_2O mixtures, conclude that water completely fills the void space, and that the silica has a density similar to that of bulk amorphous silica, within an uncertainty of about 10%. Tun *et al* chose the scattering length density of cristobalite [29], which is 4% denser than SiO_2 glass. Morineau *et al* [21] measured the temperature dependence of the density of methanol confined in 35 and 24 Å channels in MCM-41. They chose to normalize their data to the density of bulk methanol at 300 K, implying a silica density about 8% lower than bulk silica. Liu *et al* [30] performed a contrast variation experiment on MCM-41 with 15 and 19 Å diameter channels, using D_2O/H_2O mixtures, and state that a silica scattering length density of 4.006×10^{10} cm^{-2} is implied, which corresponds to a mass density about 15% larger than bulk silica. It is not obvious to us that any of these choices is optimal for our experiment, but we regard the density of bulk amorphous silica as the most credible option. We estimate the uncertainty (standard deviation) in the derived water density for these purposes is approximately 5%.

The background level needed to determine I_{wet} from scans in temperature at fixed Q was determined through the fits of figure 1. That is, the ratio of background to the diffracted peak intensity at $Q = 0.25$ Å^{-1} was noted at 270 K, and the background was thereafter assumed to be a number independent of temperature. The latter assumption seems justified, since the simultaneous fits for 11 temperatures between 170 and 270 K, using the same background, give satisfactory results. For clarity, figure 1 displays fits at only six of these temperatures.

In figure 2, we show the density as a function of temperature, derived from scans made by holding Q fixed at the peak position, and varying only temperature. As can be seen from figure 1, the position does not shift with temperature. By scanning only temperature at a fixed position, one can make maximum use of counting time to determine density changes. The number of counts in each point of this scan varies from 338 000 to 222 000, so that the error bar due to counting statistics is approximately 0.2% in the count rate, and only 0.05% in the derived density. As discussed above, other factors imply much larger uncertainties in the scale, but not in the shape, of this curve. The data in figure 2 are the average of a cooling scan at a rate of 0.1 K min^{-1}, followed by a warming scan at the same rate. The two curves are nearly identical in shape, but are shifted in temperature by about

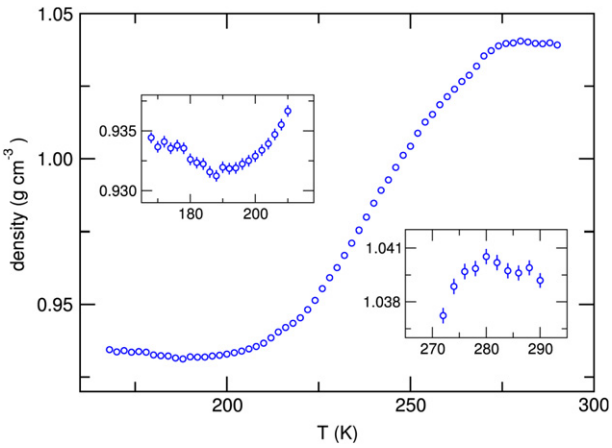

Figure 2. Density of D_2O in MCM-41-S derived from scans in temperature at $Q = 0.25$ Å^{-1}. Error bars shown in the insets are standard deviations due to counting statistics. See the text for a discussion of systematic uncertainty.

3 K. The latter does not indicate any hysteresis, but can be explained as a lag of sample temperature to the temperature measured at the cold head of the closed cycle refrigerator. We verified this explanation by monitoring intensity as a function of time after a 20 K change in set point of the temperature controller, which yielded a signal decay constant of 26 min.

The shape shown in figure 2 is similar to the observations of Liu *et al* in [20] and [30]. The insets in figure 2 show the data on an expanded vertical scale in the high and low temperature plateau regions, showing a weak density maximum at 280 K and a weak minimum at 190 K. A much deeper minimum has been observed [20] for D_2O in a MCM-41-S sample with 15 Å diameter channels, but weaker minima were seen in other samples [30]. The recent study by Mancinelli *et al* [25] questions whether the (10) peak intensity can be used as a reliable measure of adsorbed D_2O density. We believe that the strongest argument against their point of view is the observation that the (10) peak can be reduced to essentially zero intensity in a contrast variation experiment. If strong layering effects were present, this would not be possible. For example, Tun *et al* [29], referring to figures 2–4 of their paper, demonstrate that the pore space is very uniformly filled at full hydration, but partial hydration leads to a non-uniform distribution, with void spaces appearing away from the pore walls.

3.2. Higher q data—FSDP—increase in hydrogen bonding

The so-called first sharp diffraction peak (FSDP) of D_2O occurs at 2.0 Å^{-1} in the bulk liquid under ambient conditions [31], and is by far the most prominent feature in the entire diffraction pattern, representing a modulation over the average value of $S(Q)$ of more than a factor of two, while other features are less prominent by about an order of magnitude. A recent neutron diffraction study [18] of D_2O confined in MCM-41 shows the narrowing and shift of the FSDP upon cooling, in which the authors measured at four temperatures,

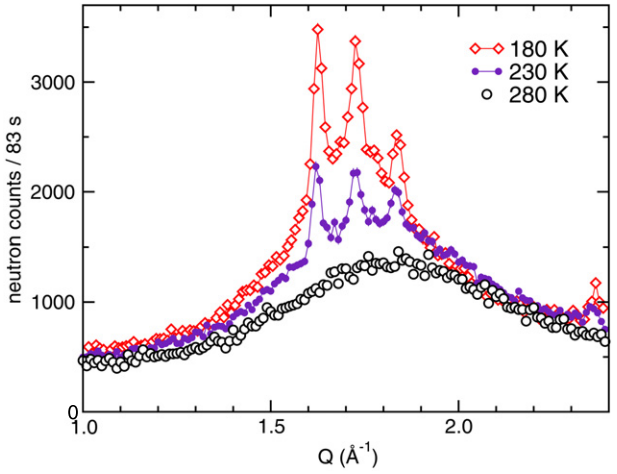

Figure 3. Scans over the FSDP region of D_2O in MCM-41S observed in our experiment at three representative temperatures. Error bars are standard deviations due to counting statistics. The sharp peaks arise from water expelled from the pores because of water expansion.

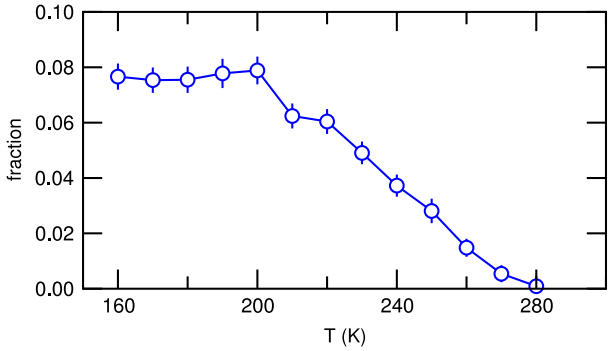

Figure 4. Fraction of the D_2O scattering intensity contained in the ice Ih Bragg peaks. See the text for details.

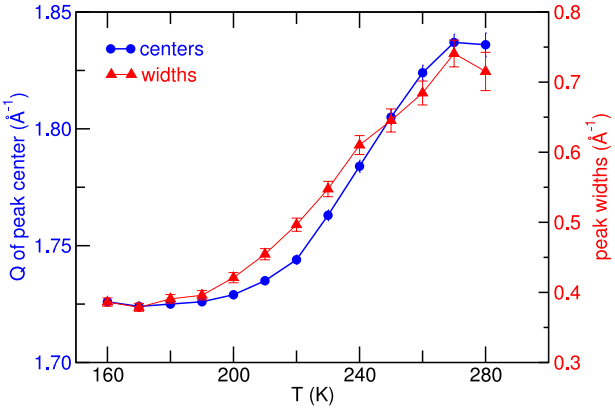

Figure 5. Positions and widths (FWHM) of Lorentzian line shapes fitted to FSDP scans, excluding ice Bragg peaks and a linear background. The errors are standard deviations estimated for the fit parameters.

298, 273, 223, and 173 K, noting the shift and narrowing apparent between the two lowest temperatures. The radial distribution functions (rdfs) derived from their data clearly show the interatomic correlations indicative of increasing hydrogen bonding on cooling, and the similarity of the 173 K structure to low-density amorphous ice (LDA) [32].

In our experiment, which covers limited Q-ranges, it is not possible to derive rdfs. However, we have obtained data at 13 temperatures between 160 and 280 K, and hence we are able to correlate the changes with simultaneous changes in density. Figure 3 shows our data on the FSDP at three representative temperatures. At 280 K, a broad peak centered at 1.84 Å^{-1} is observed. At 230 and 180 K, the peak has intensified markedly, sharpened, and shifted to lower Q. Meanwhile sharp peaks appear at 1.62, 1.72, 1.83, and 2.37 Å^{-1}, characteristic of the formation of crystalline ice Ih. It is important to note that the ice peaks arise not from excess water on the sample at room temperature, but from water expelled from the channels upon cooling. If the water were simply excess, it would freeze at 277 K, and the ice-derived intensity would show an upward jump. Instead, we see from figure 4 that it increases continuously and gradually between 270 and 200 K, reaching a plateau below 200 K. The quantity plotted in figure 4 is the ratio of the integrated intensities of the four ice peaks to the intensities of the ice peaks plus the integrated intensity of the FSDP. It is worth noting that the expulsion of water from the pores due to the density change does not seem to affect the reproducibility of the (10) Bragg peak intensity measurement. In fact, consecutive cooling and warming scans give the same results except for a shift in temperature of 3 K, as already discussed.

We note that the Bragg peaks of hexagonal ice shown in figure 3 cannot arise from water that has crystallized within the pores, since the latter would give rise to much broader peaks than the ones we observe. Specifically, microcrystalline ice confined to 20 Å channels should exhibit peak widths on the order of 0.3 Å^{-1}. Furthermore, as observed by Morishige and Kawano [19], crystallization within the pores of MCM-41-S is to a cubic form of ice, and, as we note above, is characterized by a sharper temperature dependence of the low-Q diffraction peak, rather than the smooth change observed in our experiment.

Fitting a Lorentzian to the FSDP, plus a sloping linear background, and narrow Gaussians at the ice peaks, we obtain the data shown in figure 5. The FSDP peak center shifts evenly over a 70 K transition region from a high temperature plateau above 270 K to a low temperature plateau below 200 K. The shape of this curve is very similar to that of the density, with some indication of a slight upturn at the lowest temperature. The flex point in the density versus T curve (figure 2), has been interpreted in the past as the crossing of the Widom line and the temperature at which the populations of LDL- and HDL-like water molecules is the same [33]. Within this framework, according to our data, the transition from a mostly HDL structure to a mostly LDL structure would take place at around 240 K $\pm$ 10 K, in agreement with the finding of [33]. The width of the FSDP meanwhile changes from 0.73 Å^{-1} at 280 K to 0.38 Å^{-1} FWHM at 170 K. If the widths are represented as correlation lengths ($=2\pi$/FWHM),

these vary from 8.6 Å at 280 K to 16.5 Å at 170 K. The latter number may indicate that the correlation length stops growing when it is comparable to the channel diameter, but more data would be needed to demonstrate that the correspondence has a physical origin. Morishige and Kawano [19] studied the pore size dependence of the x-ray diffraction pattern from H_2O in MCM41, with channel diameters ranging from 24 to 58 Å. Comparing the two lowest diameters, 24 and 29 Å, the width of the FSDP is indeed smaller for the larger pore diameter, but when the pore diameter exceeds 24 Å, the temperature dependence changes qualitatively, with the appearance of a sharper transition region indicating crystallization of the water in the central regions of the pores.

Given the anisotropic nature of the pores in MCM-41-S, it is possible that the correlation lengths along the channel axis change more rapidly with temperature than those in the perpendicular direction. However, our data contain no direct information about such a possibility.

4. Conclusions

Our main point is that the temperature dependences of the width and position of the FSDP (figure 5) are closely correlated with the temperature dependence of the density (figure 2). The physical origin of these variations is changing hydrogen bonding in the transition region from 190 to 280 K. At temperatures above 200 K, it is evident from quasielastic scattering measurements at 1 μeV resolution on the high flux backscattering spectrometer [4] that observable translational diffusion is present, and hence we conclude that a substantial fraction of the occluded water is in the liquid state while expansion is occurring. Describing the temperature dependence of the structure as a liquid–liquid transition is thus appropriate, but one should also bear in mind that the transformation occurs over a very wide temperature range. Water is unusual in exhibiting two well-characterized amorphous solid states at low temperature, i.e. high-density amorphous ice (HDA), and low-density amorphous ice (LDA) [3]. It is thus tempting to regard the liquid–liquid transformation as analogous to a transition between a low-density liquid (LDL) and a high-density liquid (HDL) [34]. Qualitatively, such a description is reasonable in the sense that a higher-density fluid is transforming to a lower-density one through increasing hydrogen bonding. However, the total expansion, on the order of 11%, is much smaller than the 24% difference between HDA and LDA, but comparable to the 8% change from ordinary liquid water to ice Ih. The position of the FSDP in our experiment at maximum density is 1.84 $Å^{-1}$, a significantly lower value than the position for bulk heavy water, about 2.0 $Å^{-1}$. It appears that this shift of the FSDP is induced by proximity to the hydrophilic silica walls, since it is also observed for monolayer heavy water adsorbed in Vycor porous silica glass [34]. Our data are also consistent with investigations on D_2O in MCM-41 that have reported measurements at fewer temperatures, but over much wider Q ranges [18].

The methods we have described can be implemented in a straightforward manner to the investigation of confined water at moderately high pressures, up to 0.4 GPa, using He gas as a pressure medium and a large sample volume. Such measurements are in progress.

Acknowledgments

We especially wish to thank Dr William Ratcliff for his generous assistance with the measurements. We also thank Dr Yang Zhang and Professor Sow-Hsin Chen for useful discussions.

References

[1] Chen S H and Bellissent-Funel M C 1994 *Structure and Dynamics of Water in Confined Geometry* ed M C Bellissent-Funel and J C Dore (Dordrecht: Kluwer Academic) pp 307–36
[2] Jahnert S, Chavez F V, Schaumann G E, Schreiber A, Schonhoff M and Findenegg G H 2008 *Phys. Chem. Chem. Phys.* **10** 6039–51
[3] Mishima O and Stanley H E 1998 *Nature* **396** 329–35
[4] Faraone A, Liu L, Mou C Y, Yen C W and Chen S H 2004 *J. Chem. Phys.* **121** 10843–6
[5] Xu L M, Kumar P, Buldyrev S V, Chen S H, Poole P H, Sciortino F and Stanley H E 2005 *Proc. Natl Acad. Sci. USA* **102** 16558–62
[6] Liu L, Chen S H, Faraone A, Yen C W and Mou C Y 2005 *Phys. Rev. Lett.* **95** 117802
[7] Tokushima T, Harada Y, Takahashi O, Senba Y, Ohashi H, Pettersson L G M, Nilsson A and Shin S 2008 *Chem. Phys. Lett.* **460** 387–400
[8] Mallamace F, Branca C, Broccio M, Corsaro C, Mou C Y and Chen S H 2007 *Proc. Natl Acad. Sci. USA* **104** 18387–91
[9] Huang C *et al* 2009 *Proc. Natl Acad. Sci. USA* **106** 15214–8
[10] Poole P H, Sciortino F, Essmann U and Stanley H E 1992 *Nature* **360** 324–8
[11] Sastry S, Debenedetti P G, Sciortino F and Stanley H E 1996 *Phys. Rev.* E **53** 6144–54
[12] Angell C A 2008 *Science* **319** 582–7
[13] Clark G N I, Hura G L, Teixeira J, Soper A K and Head-Gordon T 2010 *Proc. Natl Acad. Sci. USA* **107** 14003–7
[14] Huang C *et al* 2010 *Proc. Natl Acad. Sci. USA* **107** E45
[15] Soper A K 2008 *Mol. Phys.* **106** 2053–76
[16] Liu E, Dore J C, Webber J B W, Khushalani D, Jahnert S, Findenegg G H and Hansen T 2006 *J. Phys.: Condens. Matter* **18** 10009–28
[17] Webber B and Dore J 2004 *J. Phys.: Condens. Matter* **16** S5449–70
[18] Yoshida K, Yamaguchi T, Kittaka S, Bellissent-Funel M C and Fouquet P 2008 *J. Chem. Phys.* **129** 054702
[19] Morishige K and Kawano K 1999 *J. Chem. Phys.* **110** 4867–72
[20] Liu D Z, Zhang Y, Chen C C, Mou C Y, Poole P H and Chen S H 2007 *Proc. Natl Acad. Sci. USA* **104** 9570–4
[21] Morineau D, Guegan R, Xia Y D and Alba-Simionesco C 2004 *J. Chem. Phys.* **121** 1466–73
[22] Morineau D, Xia Y and Alba-Simionesco C 2002 *J. Chem. Phys.* **117** 8966
[23] Morineau D, Xia Y D and Alba-Simionesco C 2002 *J. Chem. Phys.* **117** 8966–72
[24] Xia Y D, Dosseh G, Morineau D and Alba-Simionesco C 2006 *J. Phys. Chem.* B **110** 19735–44

[25] Mancinelli R, Bruni F and Ricci M A 2010 *J. Phys. Chem. Lett.* **1** 1277–82
[26] Liu Y, Zhang W Z and Pinnavaia T J 2000 *J. Am. Chem. Soc.* **122** 8791–2
[27] Soper A K 2011 *J. Phys.: Condens. Matter* submitted (arXiv:1107.3492)
[28] Edler K J, Reynolds P A and White J W 1998 *J. Phys. Chem.* B **102** 3676–83
[29] Tun Z, Mason P C, Mansour F K and Peemoeller H 2002 *Langmuir* **18** 975–7
[30] Liu D Z, Zhang Y, Liu Y, Wu J L, Chen C C, Mou C Y and Chen S H 2008 *J. Phys. Chem.* B **112** 4309–12
[31] Narten A H 1972 *J. Chem. Phys.* **56** 5681
[32] Finney J, Hallbrucker A, Kohl I, Soper A and Bowron D 2002 *Phys. Rev. Lett.* **88** 225503
[33] Mallamace F, Broccio M, Corsaro C, Faraone A, Majolino D, Venuti V, Liu L, Mou C Y and Chen S H 2007 *Proc. Natl Acad. Sci. USA* **104** 424–8
[34] Zanotti J M, Bellissent-Funel M C and Chen S H 2005 *Europhys. Lett.* **71** 91–7